Supplementary Information

Geometrical Constraints of Thermal Dehydration of β-Calcium Sulfate Hemihydrate Induced by Self-Generated Water Vapor

Shun Iwasaki, Yuto Zushi, and Nobuyoshi Koga*

Department of Science Education, Division of Educational Sciences, Graduate School of Humanities and Social Sciences, Hiroshima University, 1-1-1 Kagamiyama, Higashi-Hiroshima 739-8524, Japan

Contents

S1. Sample Characterization s2

Figure S1. XRD pattern of the as-received calcium sulfate hemihydrate sample. s2

Figure S2. FT-IR spectrum of the as-received calcium sulfate hemihydrate sample. s2

Figure S3. SEM images of the sample particle: (a) particle shape and (b) particle surface. s2

Figure S4. EDX spectrum of the calcium sulfate hemihydrate sample. s2

S2. Thermal Behavior s2

Figure S5. Results of the HT-XRD performed in the isothermal heating program mode at 383 K in a flow of dry N_2 gas: (a) changes in the XRD pattern with heating time, (b) XRD pattern recorded in the duration of 275–300 min, and (c) changes in the crystallite sizes of the reactant (β-$CaSO_4 \cdot (1/2)H_2O$) and product (γ-$CaSO_4$) during the thermal dehydration process. s2

Figure S6. Influence of the sample mass (m_0) on the TG–DTG curves for the thermal dehydration of CS-HH in an open pan, recorded at a β of 5 K min^{-1} in a flow of dry N_2 gas (q_v = 80 cm^3 min^{-1}). s3

Figure S7. Comparison of TG–DTG curves for the thermal dehydration of CS-HH (m_0 = approximately 10.0 mg) in open and lidded pans, recorded at a β of 5 K min^{-1} in a flow of dry N_2 gas (q_v = 80 cm^3 min^{-1}). s3

S3. Formal Kinetic Analysis s3

Figure S8. Comparison of the Friedman plots at α = 0.5 for the thermal dehydration of CS-HH in open and lidded pans. s3

Figure S9. Comparison of the experimental master plots, normalized with reference to the ($d\alpha/d\theta$) value at α = 0.5, for the thermal dehydration of CS-HH in open and lidded pans. s3

S4. Physico-Geometrical Kinetic Modeling s4

Table S1. Optimized rate constants based on the SR–PBR(1) model for the thermal dehydration of CS–HH in open pan and lidded pans s4

* Corresponding author. e-mail: nkoga@hiroshima-u.ac.jp

S1. Sample Characterization

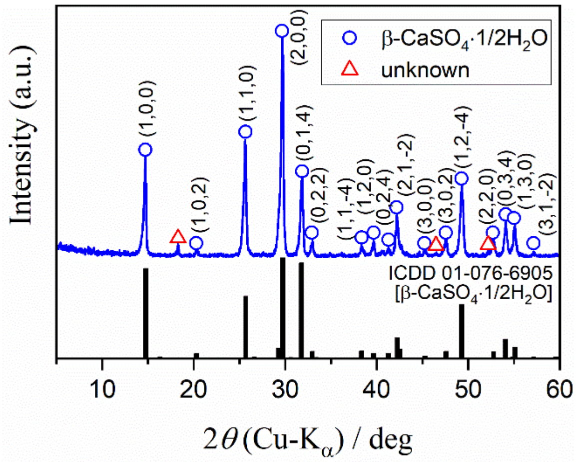

Figure S1. XRD pattern of the as-received calcium sulfate hemihydrate sample.

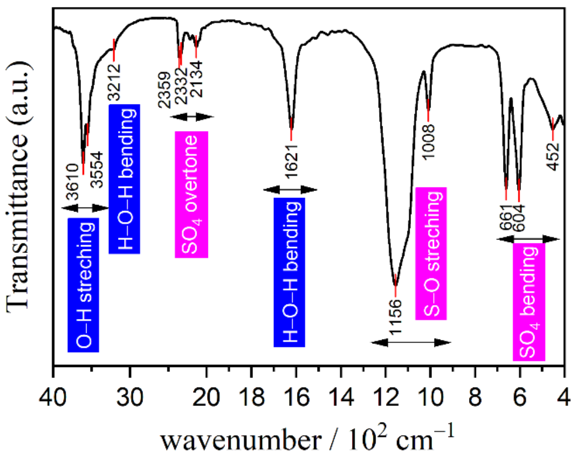

Figure S2. FT-IR spectrum of the as-received calcium sulfate hemihydrate sample.

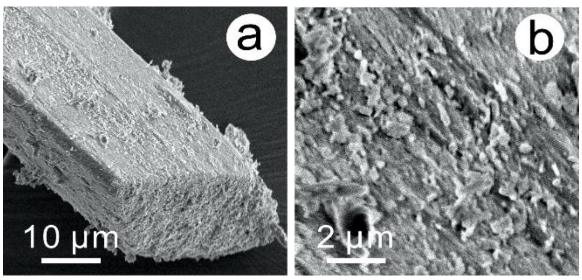

Figure S3. SEM images of the sample particle: (a) particle shape and (b) particle surface.

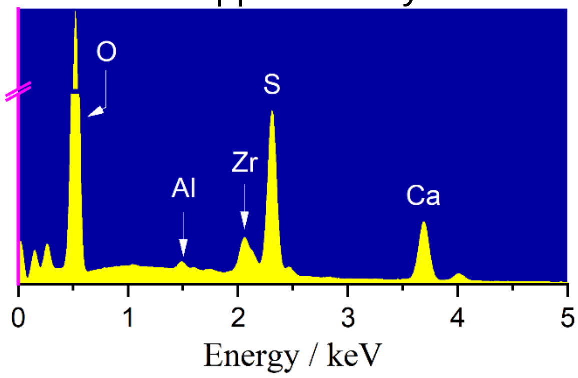

Figure S4. EDX spectrum of the calcium sulfate hemihydrate sample.

S2. Thermal Behavior

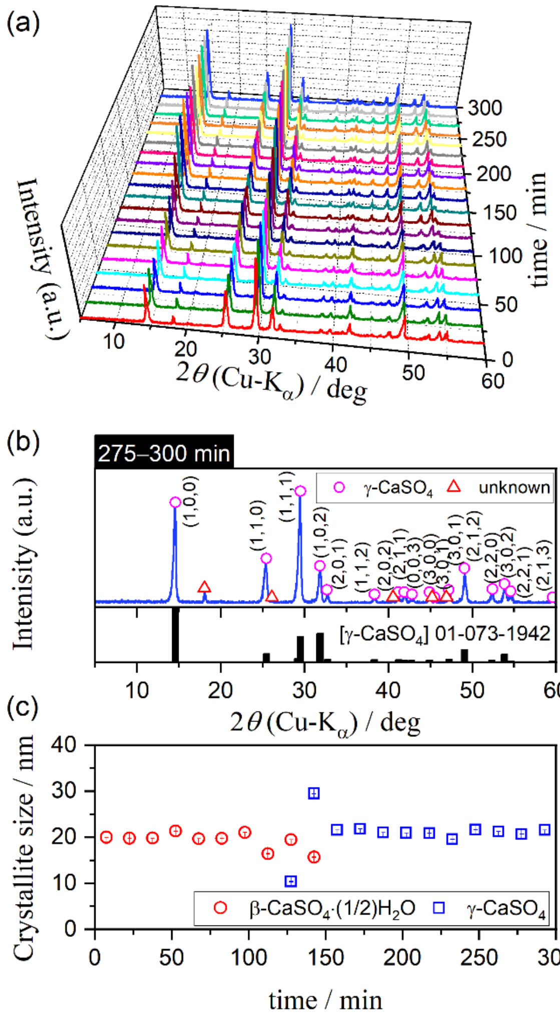

Figure S5. Results of the HT-XRD performed in the isothermal heating program mode at 383 K in a flow of dry N_2 gas: (a) changes in the XRD pattern with heating time, (b) XRD pattern recorded in the duration of 275–300 min, and (c) changes in the crystallite sizes of the reactant (β-$CaSO_4\cdot(1/2)H_2O$) and product (γ-$CaSO_4$) during the thermal dehydration process.

S3. Formal Kinetic Analysis

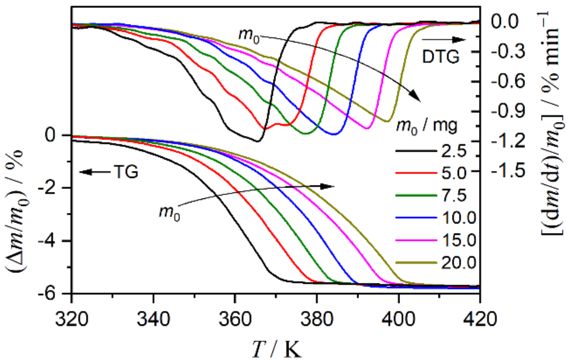

Figure S6. Influence of the sample mass (m_0) on the TG–DTG curves for the thermal dehydration of CS-HH in an open pan, recorded at a β of 5 K min^{-1} in a flow of dry N_2 gas (q_v = 80 cm^3 min^{-1}).

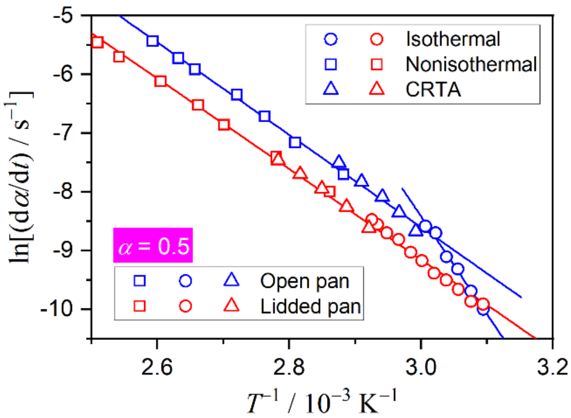

Figure S8. Comparison of the Friedman plots at α = 0.5 for the thermal dehydration of CS-HH in open and lidded pans.

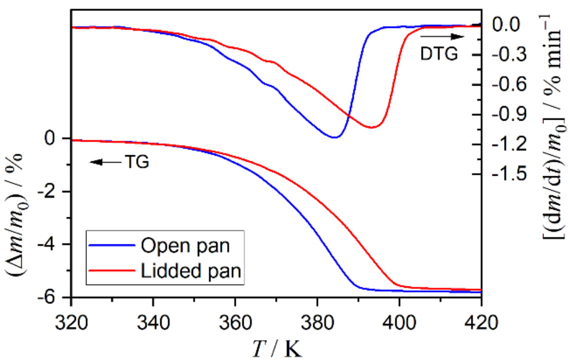

Figure S7. Comparison of TG–DTG curves for the thermal dehydration of CS-HH (m_0 = approximately 10.0 mg) in open and lidded pans, recorded at a β of 5 K min^{-1} in a flow of dry N_2 gas (q_v = 80 cm^3 min^{-1}).

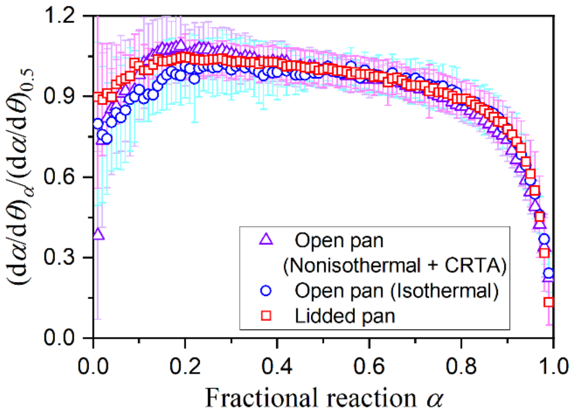

Figure S9. Comparison of the experimental master plots, normalized with reference to the $(d\alpha/d\theta)$ value at α = 0.5, for the thermal dehydration of CS-HH in open and lidded pans.

S4. Physico-Geometrical Kinetic Modeling

Table S1. Optimized rate constants based on the SR–PBR(1) model for the thermal dehydration of CS–HH in open pan and lidded pans

Sampling	T / K	k_{SR} / s^{-1}	$k_{PBR(1)}$ / s^{-1}	$R^{2, a}$	
				differential	Integral
Open pan	323.1	2.865×10^{-4}	4.461×10^{-5}	0.9882	0.9977
	325.0	7.395×10^{-4}	6.099×10^{-5}	0.9849	0.9987
	327.0	1.022×10^{-3}	8.158×10^{-5}	0.9793	0.9971
	329.0	2.294×10^{-3}	1.049×10^{-4}	0.9621	0.9984
	330.9	5.634×10^{-3}	1.568×10^{-4}	0.9628	0.9987
	333.0	9.940×10^{-3}	1.777×10^{-4}	0.9865	0.9990
Lidded pan	323.1	9.799×10^{-4}	4.854×10^{-5}	0.9769	0.9987
	325.1	1.066×10^{-3}	5.213×10^{-5}	0.9848	0.9989
	327.1	1.989×10^{-3}	6.105×10^{-5}	0.9795	0.9983
	329.0	2.502×10^{-3}	7.011×10^{-5}	0.9091	0.9976
	331.0	4.258×10^{-3}	8.335×10^{-5}	0.9583	0.9956
	333.1	5.500×10^{-3}	1.002×10^{-4}	0.9878	0.9992
	335.0	5.982×10^{-3}	1.154×10^{-4}	0.9773	0.9990
	337.0	9.936×10^{-3}	1.351×10^{-4}	0.9680	0.9992
	339.0	1.300×10^{-2}	1.564×10^{-4}	0.9835	0.9997
	340.9	1.599×10^{-2}	1.843×10^{-4}	0.9814	0.9997
	342.8	1.797×10^{-2}	2.092×10^{-4}	0.9724	0.9995

[a]Determination coefficient of the nonlinear least-squares analysis.